The International Journal of Engineering and Science (IJES)
|| Volume || 7 || Issue || 10 Ver.IV || Pages || PP 01-10|| 2018 ||
ISSN (e): 2319 – 1813 ISSN (p): 23-19 – 1805

To Study the Effect of Internal Heat Generation in Heisler's Chart

Surabhi Mahana[a], Banamali Dalai[b]
[a]*Department of Mechanical Engineering, Centre for Advanced Post Graduate Studies, BPUT, Rourkela, Odisha, 769015, India.*
[b]*Department of Mechanical Engineering, Centre for Advanced Post Graduate Studies, BPUT, Rourkela, Odisha, 769015, India.*
Corresponding Author: Surabhi Mahana

----------***ABSTRACT***----------
Study of one dimensional unsteady heat transfer in a rectangular slab with a finite length along x-direction and unit thickness along y-direction consists of development of Heisler's chart. Temperature of the slab increases due to convection heat transfer at the boundary and internal heat generation. The 1-D heat conduction equation is solved by the method of separation of variables by assuming initial fixed uniform temperature and axisymmetric boundary conditions. The eigen value of the equation is determined from the non-linear equation which is solved by the method of bisection. Heisler's chart is redeveloped for centerline temperature profile and temperature distribution at different x/L values for various Fourier numbers and Biot numbers without considering the internal heat generation. The values obtained from new chart are compared and found to be matched very well with the existing Heisler's chart. 1-D heat conduction equation is again solved by considering internal heat generation which will give a non-homogeneous equation. The non-homogeneous equation is solved by non-Fourier law. The results are plotted in the form of graphs by taking two values of internal heat generation i.e. 4.80 kw/m^3 and 120 kw/m^3. All the prepared charts are compared with existing Heisler's chart.

Keywords: *Unsteady, Conduction, Heisler's Chart, Biot number, Fourier number, Internal heat generation.*

Date of Submission: 17-10-2018 Date of acceptance: 03-11-2018

I. INTRODUCTION

Heisler's chart is a graphical tool used in conduction heat transfer problems to calculate the transient heat transfer. Instead of solving the problem numerically or analytically, the graphical tool helps to find the solution for the transient problem. This chart was first drawn by M P Heisler[1], by solving the 1-D heat transient conduction equation for symmetrical solid bodies like slab, cylinder and sphere. Later on this problem was solved by Grober[2]. These charts represent the temperature variation along the centre and various positions in the slab with variation of Biot number $\left(hx/k\right)$ and Fourier number $\left(\alpha t/L^2\right)$.

In the present analysis, considering a plane wall of thickness '2L', initial temperature 'Ti' which is assumed uniform though out the slab and the ambient temperature is T_∞. Heat transfer takes place between wall and ambient whose heat transfer coefficient is h. The plane wall is symmetrical about its centre line $(x = 0)$ and radiation effect is assumed neglected. Since the slab is symmetric, assuming a half slab, the temperature variation along the slab will be illustrated by method of separation of variables. Initially the temperature of the slab is greater than the atmosphere.

II. MATHEMATICAL FORMULATION

The following assumptions are made for the analysis:

1. Material is homogeneous and isotropic.
2. The slab is axisymmetric.
3. Thermal conductivity of the material does not vary with temperature.
4. Convective heat transfer coefficient is equal on both sides of the slab.

2.1 1-D TRANSIENT HEAT CONDUCTION EQUATION (WITHOUT INTERNAL HEAT GENERATION):

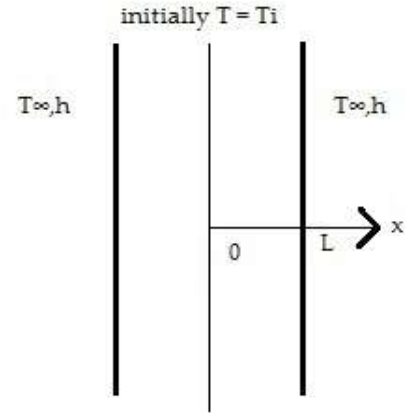

Figure1: Heat transfer on 1-D symmetrical slab.

One dimensional transient heat conduction equation for the slab (shown in Fig.1) is:

$$\frac{\partial^2 T(x,t)}{\partial x^2} = \frac{1}{\alpha}\frac{\partial T(x,t)}{\partial t} \quad \text{for } 0 < x < 1 \,\&\, t > 0 \ldots(1)$$ Initial condition

$$At\ x = 0, T(x,t) = T_i \ldots\ldots\ldots\ldots\ldots\ldots 2(a)$$

Boundary conditions are:

$$At\ \mathrm{x} = 0, \frac{\partial T(x,t)}{\partial x} = 0 \ldots\ldots\ldots\ldots\ldots\ldots 2(b)\ At\ \mathrm{x} = \mathrm{L}, -k\frac{\partial T(x,t)}{\partial x} = h(T(x,t) - T_\infty) \ldots\ldots 2(c)$$

Let $\theta(x,t) = T(x,t) - T_\infty, \theta_i = T(x,0) - T_\infty = T_i - T_\infty = \theta_i$

T = temperature (^{o}C), T_∞ = ambient temperature (^{0}C).

$$\frac{\partial^2 \theta}{\partial x^2} = \frac{\partial^2 T(x,t)}{\partial x^2}, \quad \frac{\partial \theta}{\partial t} = \frac{\partial T(x,t)}{\partial t}$$

So, the Eq.(1) can be written as:

$$\frac{\partial^2 \theta(x,t)}{\partial x^2} = \frac{1}{\alpha}\frac{\partial \theta(x,t)}{\partial t} \quad \text{for } 0 < x < 1 \,\&\, t > 0 \ldots(3)$$

And the boundary conditions are:

$$At\ \ \mathrm{x} = 0, \frac{\partial \theta(\mathrm{x},\mathrm{t})}{\partial \mathrm{x}} = 0 \ldots\ldots\ldots\ldots\ldots\ldots 4(a)\ At\ \mathrm{x} = \mathrm{L}, -k\frac{\partial \theta(x,t)}{\partial x} = h\theta(x,t) \ldots\ldots\ldots\ldots 4(b)$$

$$Let\ \ \theta(x,t) = \varphi(x)\gamma(t) \ldots\ldots\ldots\ldots\ldots\ldots (5)$$

Where $\varphi(x)$ a function depends exclusively on *x* and $\gamma(t)$ is a function depends exclusively on *t*. Then

$$\frac{\partial \theta(x,t)}{\partial t} = \varphi(x)\gamma'(t) \ldots\ldots\ldots\ldots\ldots\ldots (6)$$

$$\frac{\partial \theta(x,t)}{\partial x} = \varphi'(x)\gamma(t) \ldots\ldots\ldots\ldots\ldots\ldots (7)$$

$$\frac{\partial^2 \theta(x,t)}{\partial x^2} = \varphi''(x)\gamma(t) \ldots\ldots\ldots\ldots\ldots (8)$$

So, from equation (6), (7) and (8); Eq.(3) can be rewritten as:

$$\Rightarrow \frac{\varphi''(x)}{\varphi(x)} = \frac{1}{\alpha}\frac{\gamma'(t)}{\gamma(t)} = -\lambda^2 \ldots\ldots\ldots\ldots\ldots (9)$$ Where λ is a constant. Assuming negative sign for decaying condition. The solution of equation (9) is:

$$\frac{\varphi''(x)}{\varphi(x)} = -\lambda^2 \Rightarrow \varphi''(x) + \lambda^2\varphi(x) = 0$$

$$\Rightarrow \varphi(x) = A\cos(\lambda.x) + B\sin(\lambda.x) \ldots\ldots\ldots\ldots(10)$$ Again $$\frac{1}{\alpha}\frac{\gamma'(t)}{\gamma(t)} = -\lambda^2$$

$$\Rightarrow \gamma(t) = C_1.e^{-\lambda^2.\alpha.t} \ldots\ldots\ldots\ldots\ldots\ldots\ldots(11)$$ Where A, B and C_1 are integration constants. From equation (10) and (11), the final form of Eq.(5) is written as:

$$\theta(x,t) = [A\cos(\lambda x) + B\sin(\lambda x)]C_1e^{-\lambda^2\alpha t} \ldots..(12)$$ Applying boundary condition Eq.4(a)

$$\Rightarrow C_1e^{-\lambda^2\alpha t}\lambda(-A\sin(0) + B\cos(0)) = 0$$

$$\Rightarrow B = 0$$

Applying boundary condition equation 4(b)

$$-kC_1e^{-\lambda^2\alpha t}.\lambda[-A\sin(\lambda.L) + B\cos(\lambda.L)] =$$

$$h[A\cos(\lambda.L) + B\sin(\lambda.L)]C_1e^{-\lambda^2\alpha t}$$

$$\Rightarrow (\lambda.L)\tan(\lambda.L) = \frac{h.L}{k} = B_i$$

$$\Rightarrow \beta\tan\beta = Bi.\ldots\ldots\ldots\ldots\ldots\ldots\ldots(13)$$ Where $\beta = \lambda L$ and B_i is the Biot number. Equation (13) is nonlinear in nature which is solved by bisection method and root of the equation produces eigen value for equation (12).

Again $\theta(x,\tau) = A\cos(\lambda x)C_1e^{-\lambda^2\alpha\tau}$

Applying the initial condition Eq.(4)

$$\theta_i = A_1\cos(\lambda x)\ldots\ldots\ldots\ldots\ldots\ldots\ldots(14)$$ Where $AC_1 = A_1$. Multiplying $\cos(\lambda x)$ on both sides of Eq.(14) and integrating

$$\int_0^L \theta_i\cos(\lambda x)dx = \int_0^L A_1\cos^2(\lambda x)dx$$

$$\Rightarrow \frac{\theta_i\sin(\lambda L)}{\lambda} = A_1\left(\frac{L}{2} + \frac{\sin(2\lambda x)}{4\lambda}\right)$$

$$= A_1\left(\frac{2.L.\lambda + \sin(2L\lambda)}{4\lambda}\right)$$

$$\Rightarrow 4\theta_i\sin(\lambda L) = A_1(2L\lambda + \sin(2L\lambda))$$

$$\Rightarrow 4\theta_i\sin(\beta) = A_1(2\beta + \sin(2\beta))$$

$$\Rightarrow A_1 = \frac{4\theta_i\sin\beta}{2\beta + \sin 2\beta}\ldots\ldots\ldots\ldots\ldots\ldots(15)$$ So, $$\theta(x,t) = \frac{4\theta_i\sin\beta}{2\beta + \sin 2\beta}e^{-\lambda^2\alpha t}\cos(\lambda x)$$

For 'n' number of 'λ' values

$$\theta(x,t) = \theta_i\sum_{i=0}^{n}\frac{4\sin\beta}{2\beta + \sin 2\beta}e^{-\lambda^2\alpha t}\cos(\lambda_{n.}x)$$

$$\Rightarrow \theta(x,t) = \theta_i\sum_{i=0}^{n}\frac{4\sin\beta}{2\beta + \sin 2\beta}e^{-\beta^2\tau}\cos\left(\frac{\beta x}{L}\right) \quad \text{Where } \tau = \frac{\alpha t}{L^2}$$

$$\Rightarrow \frac{\theta}{\theta_i} = \sum_{i=0}^{n}\frac{4\sin\beta}{2\beta + \sin 2\beta}e^{-\beta^2\tau}\cos\left(\frac{\beta.x}{L}\right).....(16)$$

This equation represents the temperature distribution in the slab at different time steps and at different positions without internal heat generation.

2.2 1-D TRANSIENT HEAT CONDUCTION EQUATION WITH INTERNAL HEAT GENERATION

One dimensional transient heat conduction equation with internal heat generation 'g':

$$k\frac{\partial^2 T(x,t)}{\partial x^2}+g=\rho C_p\frac{\partial T}{\partial t}\text{..... ..... .(17)}$$

$$\Rightarrow \alpha\frac{\partial^2 T(x,t)}{\partial x^2}+\frac{g}{\rho C_p}=\frac{\partial T(x,t)}{\partial t}$$

From Eq.(17)

$$\alpha\frac{\partial^2\theta}{\partial x^2}+\frac{g}{\rho C_p}=\frac{\partial\theta}{\partial t}\text{……..……..……..(18)}$$

$$\text{Let } \theta(x,t)=\gamma(x)+\phi(x,t)\text{……..……..(19)}$$

$$\alpha[\frac{\partial^2\gamma(x)}{\partial x^2}+\frac{\partial^2\phi(x,t)}{\partial x^2}]+\frac{g}{\rho C_p}=$$

$$\frac{\partial\gamma(x)}{\partial t}+\frac{\partial\phi(x,t)}{\partial t}$$

Separating the two variables in differential equation form, it can be written as:

$$\alpha\frac{\partial^2\gamma(x)}{\partial x^2}+\frac{g}{\rho C_p}=0\text{……..……..……..(20)}$$

$$\alpha\frac{\partial^2\phi(x,t)}{\partial x^2}=\frac{\partial\phi(x,t)}{\partial t}\text{..... ....(21)}$$

Applying the boundary condition (Eq.4(a) and (b)) on Eq.(20), it can be written as:

$$x=0,\ \frac{\partial\theta}{\partial x}=0$$

$$\Rightarrow\frac{\partial}{\partial x}[\gamma(x)+\phi(x,t)]=0$$

$$\Rightarrow\frac{\partial\gamma(x)}{\partial x}=0\text{……..……..……..……..22}(a)$$

$$\text{At}\quad x=L,\ -k\frac{\partial\theta}{\partial x}=h\theta$$

$$\Rightarrow\frac{-k\partial[\gamma(x)+\phi(x,t)]}{\partial x}=h[\gamma(x)+\phi(x,t)]$$

$$-k\frac{\partial\gamma(x)}{\partial x}=h\gamma(x)\text{……..……..……..22}(b)$$

For solution of Eq.(20)

$$\alpha\frac{\partial^2\gamma(x)}{\partial x^2}+\frac{g}{\rho C_p}=0$$

$$\Rightarrow\frac{\partial^2\gamma(x)}{\partial x^2}=\frac{-g}{\alpha\rho C_p}=\frac{-g}{k}$$

$$\Rightarrow\frac{\partial^2\gamma(x)}{\partial x^2}=\frac{-g}{k}\text{..... .... (23)}$$

Integrating Eq.(23)

$$\frac{\partial\gamma(x)}{\partial x}=\int\frac{-g}{k}\partial x+C_1\text{……..……..……..(24)}$$

Applying boundary condition Eq.(22(a)) in Eq.(24)

$$C_1 = 0 \text{..... ....} (25)$$

Then Eq.(23) becomes

$$\frac{\partial \gamma(x)}{\partial x} = \frac{-g}{k} x \text{……..……..……..……..……..…..} (26)$$

Applying boundary condition Eq.(22(b)) in Eq.(26)

$$\frac{\partial \gamma(x)}{\partial x} = \frac{-g}{k} x \Rightarrow \frac{-h}{k} \gamma(L) = \frac{-g}{k} L$$

$$\Rightarrow \gamma(L) = \frac{gL}{h} \text{……..……..……..……..……..…..} (27)$$

Integrating Eq.(24)

$$\gamma(x) = \frac{-gx^2}{2k} + C_1 x + C_2 \text{..... ....} (28)$$

Using Eq.(25), (27) in Eq.(28)

$$\gamma(x) = \frac{-gx^2}{2k} + C_1 x + C_2$$

$$\Rightarrow \gamma(L) = \frac{-gL^2}{2k} + C_2$$

$$\Rightarrow \frac{gL}{h} = \frac{-gL^2}{2k} + C_2$$

$$\Rightarrow C_2 = \frac{gL}{h} + \frac{gL^2}{2k} = g.L(\frac{1}{h} + \frac{L}{2k}) \text{..... .....} (29)$$

Putting the values of C_1 and C_2 in Eq.(28);

$$\gamma(x) = \frac{g}{2}[\frac{L}{h}(2 + B_i) - \frac{x^2}{k}] \text{..... ....} (30)$$

Solution of Eq.(21) is equivalent to Eq.(11).

$$\theta(x,t) = \frac{g}{2}[\frac{L}{h}(2 + B_i) - \frac{x^2}{k}] + \theta_i \sum_{i=0}^{n} \frac{4\sin\beta}{2\beta + \sin 2\beta} e^{-\beta^2 \tau} \cos(\frac{\beta x}{L})$$

So the final solution is

$$\frac{\theta}{\theta_i} = \frac{g}{2\theta_i}[\frac{L}{h}(2 + B_i) - \frac{x^2}{k}] + \sum_{i=0}^{n} \frac{4\sin\beta}{2\beta + \sin 2\beta} e^{-\beta^2 \tau} \cos(\frac{\beta x}{L}) \text{……..…..} (31)$$

Eq.(31) represents the solution of1-D heat conduction equation along the length of a slab with internal heat generation.

$$\theta(x,t) = \frac{T(x,t) - T_\infty}{T_o - T_\infty} = \frac{T(x,t) - T_\infty}{T_o - T_\infty} \times \frac{T_o - T_\infty}{T_i - T_\infty}$$

$$= \frac{T(x,t) - T_\infty}{T_o - T_\infty} \times \theta_o$$

$$\Rightarrow \frac{\theta}{\theta_o} = \frac{T(x,t) - T_\infty}{T_0 - T_\infty} \text{..... ....} (32)$$

Where $\theta_0 = \frac{T_o - T_\infty}{T_i - T_\infty}$ = Temperature of the slab at $x = 0$. To plot the graph for temperature distribution (i.e. θ/θ_o Vs Fourier no(τ)) at different 'x/L' values Eq.(31) is used.

III. RESULT AND DISCUSSION

The Heisler's[1] chart consists of temperature at the central region of slab with variation of time which is expressed by a non-dimensional Fourier number ($\tau = \alpha t / L^2$). In the present construction of the first chart (Fig.1), the Fourier number is taken along *x*-axis and the temperature ratio θ / θ_i is taken along *y*-axis for centerline temperature profile at different $1/B_i$ values which are computed using Eq.(16). For second chart (Fig.2), $1/B_i$ is taken along *x*-axis and θ / θ_0 is taken along *y*-axis for temperature distribution at different *x*/L values. Comparison is made between present computed values (using Eq.(16)) and existing Heisler's[1] chart values at some of the Fourier numbers and $1/B_i$ values which are presented in Table.1 and Table.2 respectively.

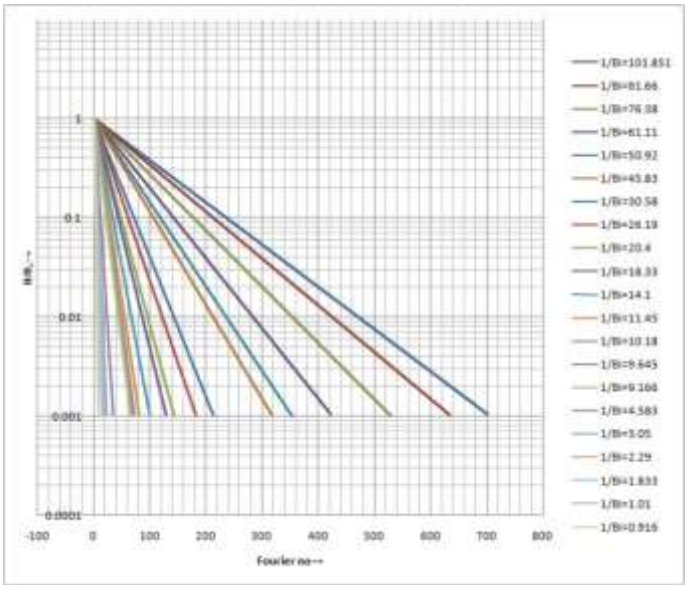

Figure-1 Shows the developed chart using Eq.(16).

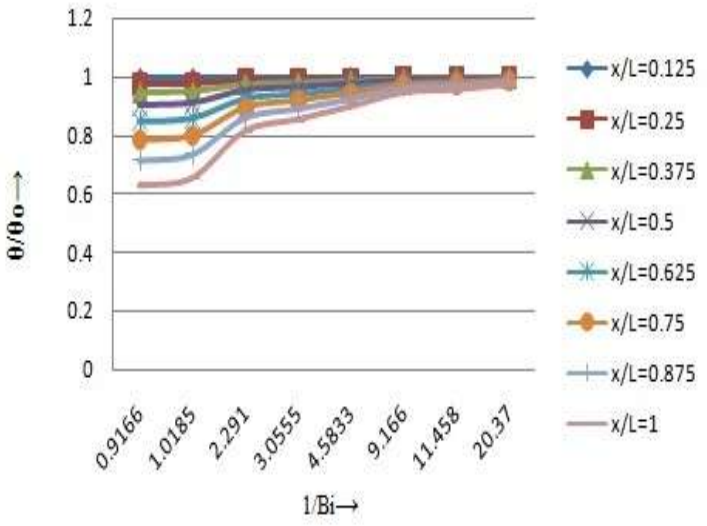

Figure-2 Shows temperature distribution for different *x*/L values at τ =3.39 using Eq.(16).

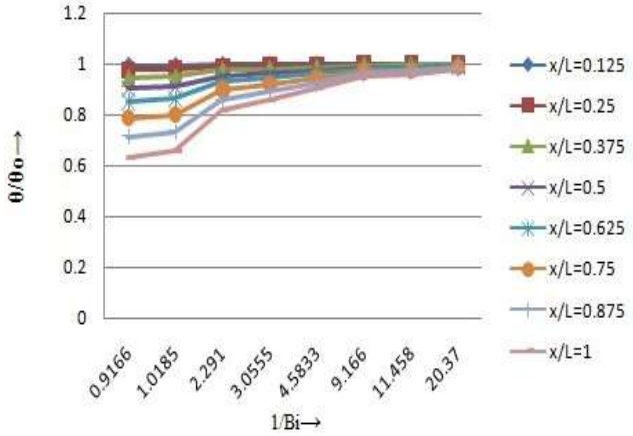

Figure-3 Shows temperature distribution fort different *x*/L values at $\tau = 8.475$ using Eq.(16).

From Table.1 and 2, it is observed that the computed values match very well with the existing Heisler's[1] chart values. In the present chart (Fig.1) the Fourier number is extended up to 700 and the $1/B_i$ is taken up to 101 for centerline temperature profile. In the results in figure 1, the *y*-axis is taken as semi-log scale and the *x*-axis is the normal coordinate axis. The temperature distribution for different *x*/L values with variation of $1/B_i$ from 0.9166 to 20.37 is shown in figure 2. In this chart both the axes are in linear scale.

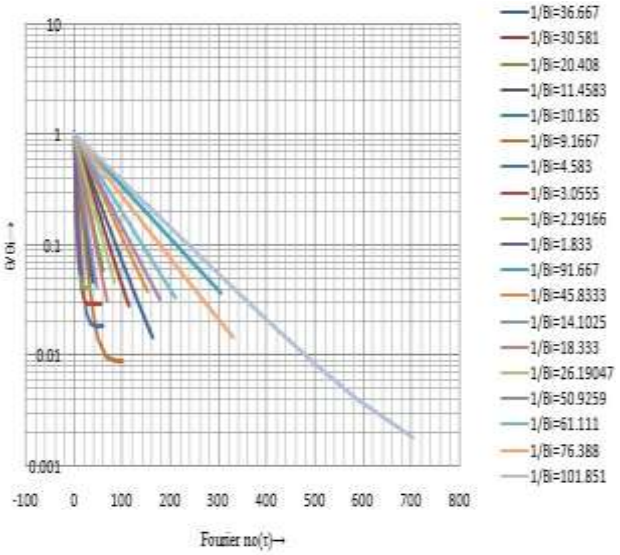

Figure-4 Shows centerline temperature distribution with internal heat generation (g=4.8 kw/m^3)

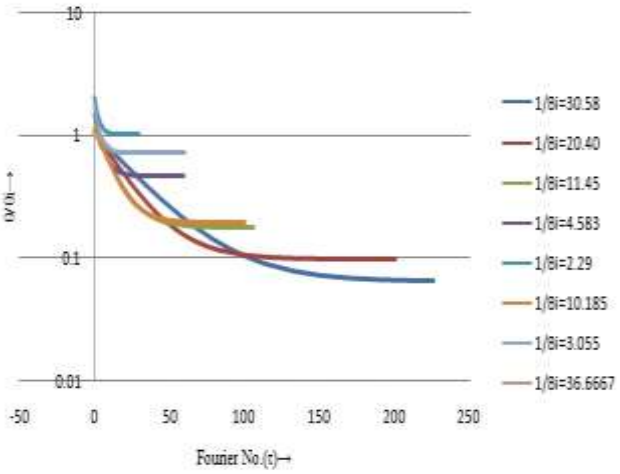

Figure-5 Shows centerline temperature distribution with internal heat generation (g=120 kw/m^3)

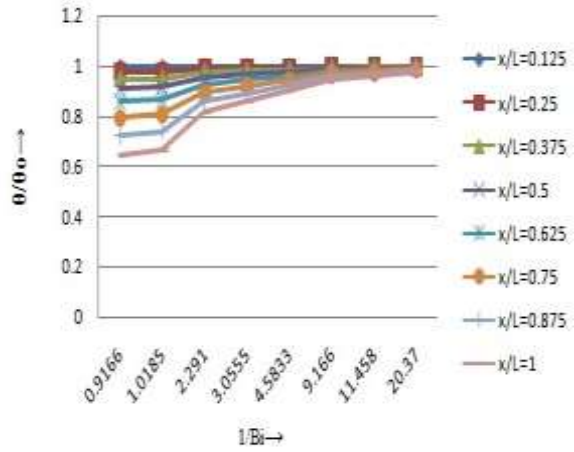

Figure-6 Shows temperature profile for different x/L values with internal heat generation (g = 4.8 kw/m^3) at τ = 3.39

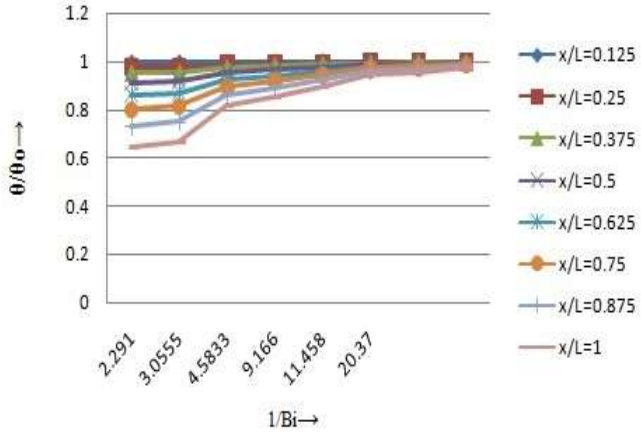

Figure-7 shows temperature profile for different x/L values with internal heat generation (g = 4.8 kw/m^3) at τ = 8.475

Next a new chart (Fig.4 & 5) is developed considering internal heat generation (g kw/m^3) for same construction of centerline temperature along *y*-axis at different Fourier numbers along *x*-axis for different constant $1/Bi$ values using Eq.(31). Similarly, figure 6 and 7 represent the non-dimensional temperature θ/θ_0 values along *y*-axis and $1/Bi$ values along *x*-axis for various constant *x*/L values which are computed using Eq.(31). Table.3 and 4 presents the comparison between the existing Heisler's[1] chart value and respective computed values in both cases (with and without internal heat generation). In figure 2 & 6 and 3 & 7 the Fourier number are fixed at 3.39 and 8.475 respectively.

Table:1 Comparison between Heisler's[1] chart value and computed present chart value.

L	1/Bi	Fourier No (τ)	θ/θ_i (Heisler[1])	θ/θ_i (Present)
0.01	91.667	508.5	0.004	0.004
0.012	76.388	470.8	0.002	0.002
0.015	61.111	300	0.008	0.008
0.018	50.925	314	0.002	0.002
0.030	30.555	2.260	0.960	0.962
0.045	20.370	1.004	0.979	0.980
0.050	18.333	108.48	0.003	0.003
0.065	14.102	80.230	0.005	0.005
0.100	1.166	2.034	0.779	0.780
0.300	3.055	0.904	0.820	0.820
0.400	2.291	1.141	0.680	0.681
0.500	1.833	10.848	0.007	0.007
0.900	1.018	4.018	0.060	0.060

Table-2 comparison between values obtained from existing chart and values obtained from computed charts at $\tau = 3.39$ and $\tau = 8.475$.

x/L	1/Bi	θ/θ_0 Heisler [1]chart	θ/θ_0 (Present, $\tau = 3.39$)	θ/θ_0 (Present, $\tau = 8.475$)
1	2.291	0.8200	0.8160	0.8162
1	4.583	0.8600	0.8501	0.8501
1	11.458	0.9700	0.9579	0.9579
0.875	2.291	0.8600	0.8581	0.8581
0.875	3.055	0.8610	0.8498	0.8498
0.875	11.458	0.9700	0.9677	0.9677
0.75	2.291	0.9100	0.8950	0.8950
0.75	3.055	0.9210	0.9183	0.9183
0.75	20.370	0.9870	0.9860	0.9860
0.625	2.291	0.9300	0.9267	0.9267
0.625	3.055	0.9400	0.9430	0.9430
0.625	20.370	0.9900	0.9905	0.9905

From figure 4 and 5, considering the effect of internal heat generation on temperature profile, it is observed that the values obtained for temperature profile are more than the values obtained without internal heat generation at a particular instant of time. It shows the effect of internal heat generation on the change in temperature with respect to time and positions. When internal heat generation is small i.e. g=4.80 kw/m^3 the difference in temperature is slightly greater than the temperature without internal heat generation case. But when the 'g' value is more *i.e*. 120 kw/m^3 the difference is appreciable. Also it can be seen that the values with internal heat generation, the temperature decreases with increase in time upto a certain period of time but after that time period is over, the temperature becomes constant which clearly shows the effect of internal heat generation. This time period decreases with increase of internal heat generation as shown in figure 5.

Table-3 Comparison of computed values obtained Eq.(16) with Eq.(31) at two different internal heat generation (g = 4.8 kw/m^3) and (g = 120 kw/m^3).

L	1/Bi	(τ)	θ/θ_i (Heisler[1])	θ/θ_i (present)	θ/θ_i (g = 4.8 kw/ ^{3}	θ/θ_i (g=120 kw/m^3
0.030	30.58	4	0.86	0.863	0.8710	0.932
0.030	30.58	10	0.71	0.710	0.7200	0.850
0.030	30.58	20	0.51	0.510	0.5200	0.580
0.030	30.58	40	0.28	0.280	0.2900	0.480 (const)
0.030	30.58	80	0.07	0.070	0.0800	0.480
0.045	20.40	4	0.83	0.832	0.8350	0.900
0.045	20.40	10	0.62	0.620	0.6250	0.700
0.045	20.40	20	0.38	0.380	0.3880	0.480
0.045	20.40	40	0.14	0.142	0.1500	0.230
0.045	20.40	60	0.04	0.040	0.0500	0.160 (const)
0.080	11.45	10	0.44	0.440	0.4500	0.580
0.080	11.45	20	0.18	0.180	0.2000	0.350
0.080	11.45	40	0.03	0.030	0.0350	0.200
0.080	11.45	60	0.007	0.007	0.0085	0.180 (const)

Table-4 Comparison between values obtained from Heisler's[1] chart and computed charts at $\tau = 3.39$ and $\tau = 8.475$ with g = 4.8 kw/m^3.

x/L	1/Bi	θ/θ_0 (Heisler's [1] chart)	θ/θ_0 (Prese nt with g = 4.8 kw /m^3 chart) (τ =3.39)	θ/θ_0 (Prese nt with g= 4.8 kw/m^3 chart) (τ = 8.475)
1	2.291	0.820	0.8166	0.8165
1	4.583	0.860	0.8500	0.8668
1	11.458	0.970	0.9579	0.9579
0.875	2.291	0.860	0.8587	0.8581
0.875	3.055	0.861	0.8595	0.8593
0.875	11.458	0.970	0.9677	0.9677
0.750	2.291	0.920	0.8956	0.8950
0.750	3.055	0.921	0.9184	0.9183
0.750	20.370	0.980	0.9701	0.9764
0.625	2.291	0.930	0.9271	0.9267
0.625	3.055	0.940	0.9431	0.9430

0.625	20.370	0.990	0.9905	0.9905

IV. CONCLUSION

The analytical solution for the transient temperature distribution in the symmetric slab has been presented in the form of chart. Charts are presented considering without and with internal heat generation (g=4.8 kw/m^3 and 120 kw/m^3). These charts have the flexibility to compute the values at various Fourier numbers and Biot numbers. Temperature profiles obtained considering with internal heat generation are slightly higher than the without internal heat generation and this also changes with changing values of internal heat generation.

REFERENCES

[1]. M. P. Heisler. "Temperature Charts for Induction and Constant Temperature Heating." ASME Transactions 69(1947), pp.227-36.
[2]. H. Grober, S. Erk, and U. Grigull. Fundamentals of Heat Transfer. New York: McGraw-Hill, 1961
[3]. E. L. Dowty, Generalized Solutions For Transient Heat Conduction With Variable Conductivity, Nuclear Engineering And Design 6(1967) 57-64, North Holland Publishing Company, AMSTERDAM
[4]. Holman J. P., Heat Transfer, McGraw-Hill Book Company, New York, 1976
[5]. W. C. Sha and E. N. Ganic, Transient Heat Conduction at Low Biot Numbers: A Supplement to Heisler's Charts, Letters In Heat and Mass Transfer Vol.8, pp. 379-395, 1981©Pergamon Press Ltd. Printed in the United States.
[6]. Kenneth R. Diller, Modeling of Bio heat transfer processes at High and Low Temperatures, 1992 by academic press. inc.
[7]. Yunus Cengel and Ghajar, Heat and mass transfer text book, McGraw-Hill Book Company, New York.2007.
[8]. Arash Bastani, Faribortz Haghighat, Expanding Heisler chart to characterize heat transfer phenomena in a building envelope integrated with phase change materials, www.elsevier.com/locate/enbuild, www. elsevier.com/locate/enbuild,2015
[9]. Antonio Campoa, Jane Y. Chang, Facile prediction of total heat transfer from simple solid bodies to neighboring fluids: A viable alternative to Grober's charts, www.elsevier.com /locate/ apthermeng,2015.

Surabhi Mahana " To Study the Effect of Internal Heat Generation in Heisler's Chart. "The International Journal of Engineering and Science (IJES),), 7.10 (2018): 01-10